Compact Reconfigurable Matching Network for Antenna Detuning Mitigation in Smart Surfaces

Joryan Sennesael, Kamil Yavuz Kapusuz, Sam Lemey, Patrick Van Torre, and Hendrik Rogier
IDLab-Electromagnetics group, Department of Information Technology, Ghent University-imec
Ghent, Belgium (Joryan.Sennesael@UGent.be)

***Abstract*—To address the specific design challenges posed by the Internet of Things (IoT), a compact reconfigurable matching network (RMN) is designed to mitigate detuning of smart-surface-integrated antennas. The RMN is based on a third-order Chebyshev topology, composed of quarter-wavelength stubs, having a well-decoupled varactor at the end of the three shunt stubs. The circuit is designed to mitigate the impedance mismatch between a power amplifier and an antenna being detuned by objects in its reactive near field. The low-loss transmission of the circuit is tuned by controlling the varactor voltages, thereby ideally guaranteeing a low reflection coefficient at all times. Moreover, a systematic investigation of the different loss contributions is performed by means of full-wave simulations that are verified by TRL-calibrated two-port measurements. The RMN is fabricated on a 0.25-mm-thick I-TERA substrate, exploiting printed circuit board (PCB) technology, occupying 20 mm × 10 mm. Measurement results show that the RMN has a minimum insertion loss of 1.83 dB over the [5.15-5.85] GHz band. Finally, the proposed RMN is validated by correcting a detuned antenna in eleven different representative IoT scenarios, herein optimizing the transducer gain while keeping the input matched at all times.**

***Index Terms*—Antenna co-design, component characterization, Internet of Things (IoT), reconfigurable matching network, smart surfaces.**

I. Introduction

In recent years, giant leaps have been made in the connectivity of devices and assets for home automation and industrial settings. This vision, widely known as the Internet of Things (IoT), seamlessly integrates smart functionalities into everyday objects. However, it remains crucial that the operation of these smart objects is guaranteed in a wide range of, often challenging, deployment conditions.

Incorporating antennas in a smart surface [1] poses many challenges, one of them being the impedance-detuning as a result of objects or people within their reactive near field. Although antennas can be optimized to function in such integration scenarios, changes to those environments may still result in the antenna being detuned. Overseeing such impedance mismatch not only impacts antenna performance but also degrades the load-pulling effectiveness of RF amplifiers [2] or even damages them [3]. Thus, merely increasing the transmission power could have adverse effects and may be in violation of effective isotropic radiated power (EIRP) and specific absorption rate (SAR) regulations. Instead, the antennification [4] of objects demands for adaptive impedance matching networks that are able to counteract antenna mismatch and optimize communication between IoT devices.

In literature, many reconfigurable matching networks and filters have been proposed to counteract impedance detuning or to modify operating frequencies. Various solutions, including PIN diodes [5], MEMS-based circuits [6] and CMOS ICs [7], have been explored, each with their own trade-offs in terms of losses, cost, and tunability. Alternatively, varactor diodes strike a good balance between tunability and cost-effectiveness [8].

In this paper, a low-cost impedance tuner is proposed for compact integration with smart-surface-integrated antennas. This work presents a thorough study of the loss mechanisms by means of an improved simulation model. Furthermore, a practical presentation of the usable tuning range is proposed by computing the transducer gain [2] of the matching network for any load on the Smith chart, under the additional condition that the input of the network remains matched. This analysis proves that the proposed system is able to keep its input matched for any given load impedance, achieving transducer gains above -3 dB within a large region of the Smith chart. Finally, the network is connected to an air-filled substrate-integrated-waveguide (AFSIW) antenna, which is detuned by a range of different objects. The experiment proves that the RMN is able to keep its input matched, while optimizing the power transfer into the complex load impedance. In addition to our work in [9], where the RMN and its biasing electronics are co-designed with a desk-integrated AFSIW antenna, we now investigate the loss and transducer gain over the complete frequency band in more detail.

II. Description of system and loss analysis

A tunable matching network is designed for smart surface applications, providing good input impedance matching ($|S_{11}| <$ -10 dB), even when the antenna is affected by objects in its reactive near field, such as illustrated in Fig. 1. This improves the operation of the amplifier and protects it from high Voltage-Standing Wave Ratios (VSWR) in the targeted 5-GHz bands of the IEEE 802.11 standard between 5.15 GHz and 5.85 GHz. Furthermore, the transducer gain can be optimized to achieve a better power transfer to the antenna or to achieve finer control over its EIRP.

The proposed circuit is designed from a third-order Chebyshev band-pass topology with a 50% fractional bandwidth at 5.5 GHz and a 0.1 dB pass-band ripple [2]. The filter

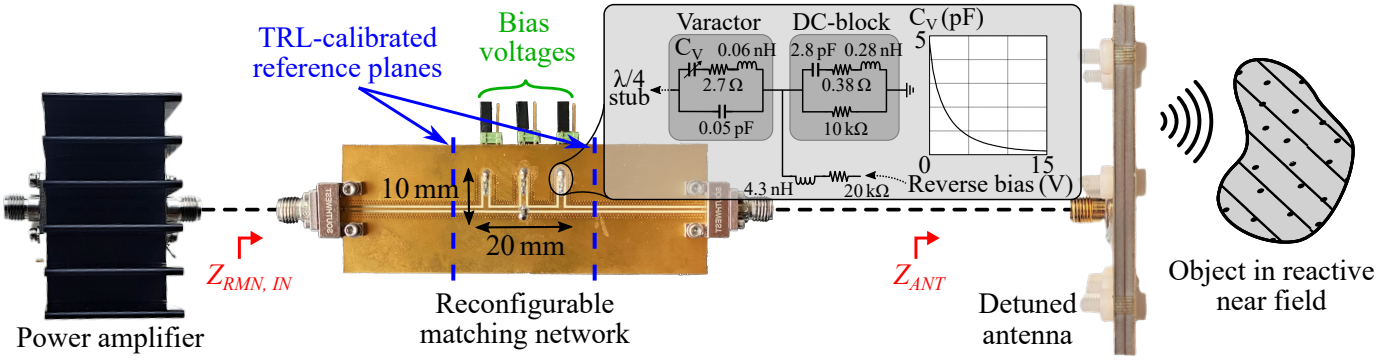

Fig. 1: Representative application with the RMN used to mitigate the impedance mismatch of a surface-integrated antenna that is detuned by objects in its reactive near field. Equivalent circuit of varactor and decoupling shown as a sub-figure.

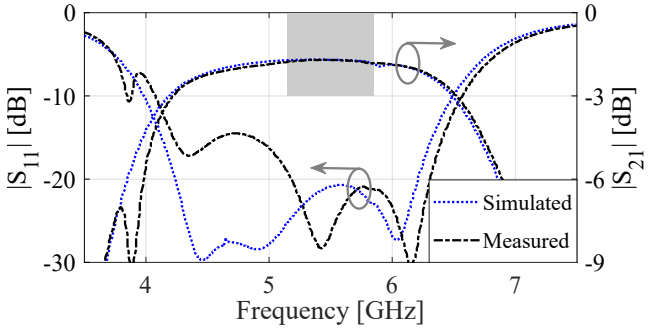

Fig. 2: Simulated and measured return loss and insertion loss of the de-embedded prototype at the nominal bias point (0 V applied at all varactor stubs) with both ports terminated by 50 Ω. Gray area marks band of interest [5.15-5.85] GHz.

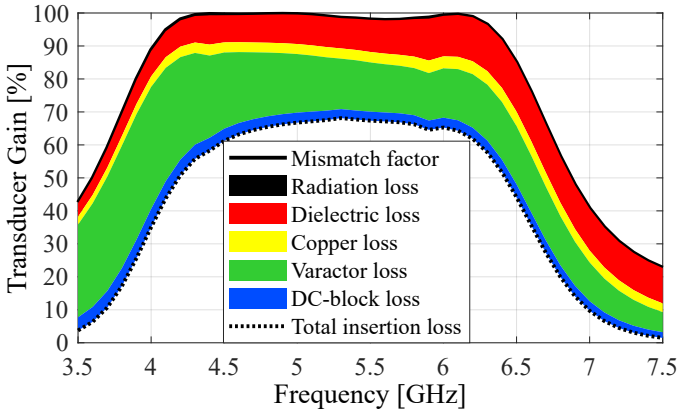

Fig. 3: Simulated individual loss mechanisms of the RMN's transducer gain at the nominal bias point (0 V applied at all varactor stubs) with both ports terminated by 50 Ω.

is implemented using shorted $\lambda/4$ transmission-line stubs in grounded co-planar waveguide (GCPW) technology on a 0.25-mm-thick I-Tera substrate ($\epsilon_r = 3.43$, $\tan\delta = 0.014$ at 5.5 GHz). Subsequently, MPV1965 varactors are incorporated in the three shunt stubs and well-decoupled by a DC-blocking capacitor, allowing the filter to operate as a tunable matching network. An updated, more accurate compared to [9], model of the parasitics is shown in Fig. 1.

The circuit is de-embedded by means of a thru-reflect-line (TRL) calibration and characterized through automated two-port S-parameter measurements over its entire frequency range for all varactor bias configurations. By judiciously identifying the discrete component's parasitics, a good agreement between simulation and measurement data is achieved, as shown in Fig. 2. At the nominal varactor biasing (0 V applied at all varactor stubs), a wide fractional impedance bandwidth of 46% is measured, closely resembling the design specifications. Furthermore, a low insertion loss of maximally 1.83 dB, corresponding to a 66% transducer gain, is measured over the entire band of interest. Leveraging the full-wave CST Microwave Studio simulation model, a detailed insight in the individual loss mechanisms of the impedance tuner is obtained over the complete frequency range, indicating that the varactors' series resistance is the main loss-contributor, as shown in Fig. 3. To maximize the power transfer through the impedance tuner into any given complex load, the varactor configuration should be optimized to achieve the maximal transducer gain. Additionally, the input of the tuner must remain matched to avoid reflections at the amplifier side. To this end, Fig. 4 shows the maximum achievable transducer gain for 5.15 GHz, 5.5 GHz and 5.85 GHz for any load impedance on the Smith chart, under the additional constraint that the input port remains matched to the 50 Ω amplifier output. At the center of the Smith chart ($Z_{ANT} = 50\,\Omega$), minimal losses of 1.83 dB can be verified over the entire frequency band. In contrast, at the edges of the Smith chart, the transducer gain theoretically becomes zero. However, in that case the optimization method can exploit the lossy nature of the varactor diodes to keep the input matched, which has been tested up to 17 dBm of input power.

III. Detuned Antenna Application

To showcase the operation of the impedance tuner in a real-life scenario, the input impedance of an AFSIW antenna (Z_{ANT} in Fig. 1) was detuned by a range of different objects, as can be seen in Fig. 5 (a), (c) and (e) at 5.15 GHz, 5.5 GHz and 5.85 GHz, respectively. This detuning is mitigated by the proposed impedance tuner, as shown by the optimized tuner input impedances ($Z_{RMN,IN}$ in Fig. 1) in Fig. 5 (b), (d) and (f), respectively. In all tested scenarios, the tuner is able to achieve a low reflection coefficient at its input ($|S_{11}| < -10$ dB),

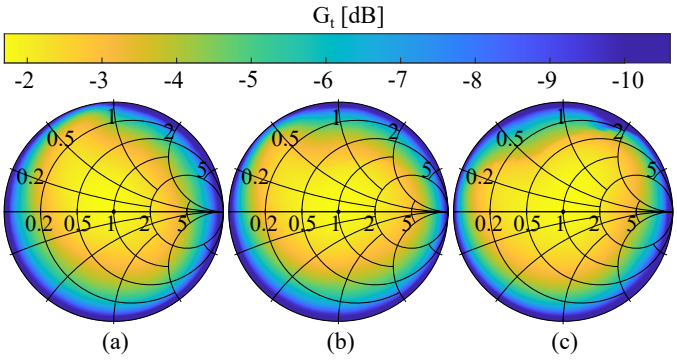

Fig. 4: Transducer gain of tuned RMN into any given load impedance on the Smith Chart, under the condition that the input remains matched ($|S_{11}| <$ -10 dB, w.r.t. 50 Ω) at (a) 5.15 GHz, (b) 5.5 GHz and (c) 5.85 GHz.

as can be verified by all of the tuned impedances lying within the VSWR < 2 circle. The average transducer gain achieved during these tests over all frequencies was -2.60 dB (55%), with the minimum being -5.17 dB (30%) for the soda can directly placed on the antenna aperture, thereby reflecting most power. Finally, for this smart-surface scenario, the matching network can be co-designed with the antenna and biasing electronics without deteriorating the system performance [9], allowing for low-cost, compact and adaptive integration scenarios.

IV. Conclusion

This work introduced a compact and reconfigurable matching network designed for the [5.15-5.85] GHz band to mitigate the impedance mismatch of an antenna disturbed by objects in its reactive near field. Measurements prove that the nominal insertion loss of the network remains below 1.83 dB over the entire band of interest. A judicious simulation model is used for a detailed loss analysis, providing insight into the individual, frequency-dependent loss mechanisms. Furthermore, it is shown that a good transducer gain can be obtained for a large portion of load impedances on the Smith chart and that the tuner can keep the amplifier matched even when the antenna reflects all power, protecting the amplifier in that case. The proposed system is deployed in a representative application scenario, correcting the impedance mismatch of a detuned AFSIW antenna by a range of objects and achieving an average transducer gain of -2.60 dB. Finally, the design allows for a complete AFSIW antenna-integration, offering elegant co-design possibilities.

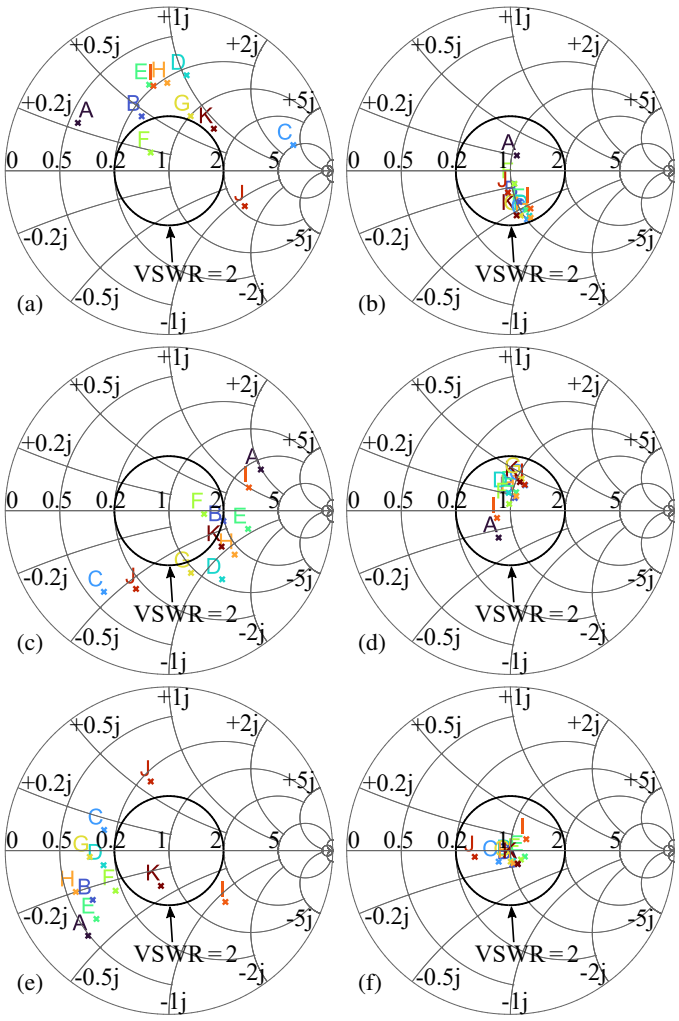

Fig. 5: Input impedance of stand-alone detuned antenna (a), (c), (e), by objects in its reactive near field compared to input impedance of optimized RMN connected to detuned antenna (b), (d), (f), at 5.15 GHz, 5.5 GHz and 5.85 GHz, respectively. Test objects directly placed on antenna aperture: flash drive (A), coffee mug (B), soda can (C), laptop (D), smartphone (E), computer mouse (F) and keyboard (G), hand (H), water bottle (I). Test objects 18 mm above antenna: water bottle (J), aluminium sheet (K).

References

[1] L. Roselli *et al.*, "Smart Surfaces: Large Area Electronics Systems for Internet of Things Enabled by Energy Harvesting," *Proc. IEEE*, vol. 102, no. 11, pp. 1723–1746, 2014. doi: 10.1109/JPROC.2014.2357493

[2] D. Pozar, *Microstrip Engineering*. Hoboken, NJ, USA: Wiley, 2004.

[3] Y. Zhang *et al.*, "A Low-Power Reflection-Coefficient Sensor for 28-GHz Beamforming Transmitters in 22-nm FD-SOI CMOS," *IEEE J. Solid-State Circuits*, vol. 56, no. 12, pp. 3704–3714, 2021. doi: 10.1109/JSSC.2021.3106700

[4] P. Avaltroni, S. Nappi, and G. Marrocco, "Antennifying Orthopedic Bone-Plate Fixtures for the Wireless Monitoring of Local Deep Infections," *IEEE Sensors J.*, vol. 21, no. 18, pp. 21 012–21 021, 2021. doi: 10.1109/JSEN.2021.3097448

[5] J.-X. Xu, Y.-M. Xue, L. Gao, and X. Y. Zhang, "Switchable Filtering Circuit with Single- and Multi-Channel Operations," *IEEE Trans. Circuits Syst. II*, vol. 67, no. 12, pp. 2958–2962, 2020. doi: 10.1109/TCSII.2020.2993234

[6] R. G. Pesel, S. S. Attar, and R. R. Mansour, "MEMS-Based Switched Capacitor Banks for Impedance Matching Networks," in *Eur. Microw. Conf.*, Paris, France, 2015, pp. 1018–1021. doi: 10.1109/EuMC.2015.7345939

[7] P. Sjoblom and H. Sjoland, "Measured CMOS Switched High-Quality Capacitors in a Reconfigurable Matching Network," *IEEE Trans. Circuits Syst. II*, vol. 54, no. 10, pp. 858–862, 2007. doi: 10.1109/TCSII.2007.901629

[8] J. A. Estrada, S. Johannes, D. Psychogiou, and Z. Popovic, "Tunable Impedance-Matching Filters," *IEEE Microw. Wireless Compon. Lett.*, vol. 31, no. 8, pp. 993–996, 2021. doi: 10.1109/LMWC.2021.3083184

[9] J. Sennesael, K. Y. Kapusuz, S. Lemey, P. V. Torre, and H. Rogier, "Compact AFSIW Antenna with Integrated Digitally Controlled Impedance Tuner for Smart Surfaces," *IEEE Trans. Circuits Syst. II*, pp. 1–1, 2023. doi: 10.1109/TCSII.2023.3319081